A COUPLED FDM-MPM METHOD FOR MODELING MULTIPLE PHENOMENA OF FLUID AND AND SOIL

Yota Enomoto[1] and Taro Arikawa[2]

This study proposes an advanced analytical framework for investigating soil behavior under hydraulic loading by establishing a coupled soil–water analysis that discretizes fluid flow using the Finite Difference Method (FDM) and soil deformation using the Material Point Method (MPM). Numerical methods for coupled soil–water analysis can generally be classified into grid-based approaches (e.g., the Finite Element Method, FEM) and particle-based approaches (e.g., the Distinct Element Method, DEM). Grid-based approaches often encounter difficulties in dealing with large deformations and collapse phenomena, whereas particle-based approaches can be computationally expensive and may struggle to accurately capture seepage. To overcome these limitations, a coupled fluid–soil analysis model has been developed using MPM, an intermediate method that combines strengths from both grid- and particle-based techniques. The model has been applied to a two-dimensional consolidation and seepage problem. The results indicate that the proposed method can accurately reproduce large deformations and seepage—phenomena that pose challenges for traditional grid-based methods—while also aligning well with earlier findings from particle-based analyses.

Keywords: fluid-soil interaction, large deformation problems, seepage problem, numerical analysis, MPM,

Introduction

In FEM analyses, large deformations cause significant distortion of finite elements, rendering the analysis infeasible. Even when employing finite deformation frameworks such as the Total Lagrangian or Updated Lagrangian methods, excessive element distortion prevents continued computation and fails to capture discontinuous behaviors—including collapse and post-collapse phenomena. In cases where moderate deformations can be analyzed, the accuracy of Gaussian integration at the integration points deteriorates with increasing element distortion, causing a substantial decline in the overall reliability of the results.

Despite these challenges, FEM remains the most advanced technique for applying elastoplastic constitutive models to geotechnical materials. It can accurately capture soil behavior at small strain levels (a few percent), as evidenced by Cam-Clay–type models, the anisotropic formulations of Sekiguchi and Ota (1977), and the upper- and lower-load-surface SYS Cam-Clay models proposed by Asaoka et al. (2000). However, this is still within the realm of relatively small soil deformation, and even minute deformations can alter confining pressures and soil strength. Without accounting for such geometric nonlinearity, it is difficult to accurately simulate large deformations using FEM.

In contrast, DEM can reproduce discontinuous behaviors, but it requires modeling each soil particle and the interparticle interactions (e.g., using springs and dashpots). This approach becomes extremely computationally intensive when analyzing large-scale systems. Moreover, the interaction forces themselves must be calibrated with soil test data from field investigations. Original DEM formulations also struggle to represent porewater behavior, necessitating additional coupling methods. For instance, Kinoshita et al. (1994) integrated Darcy's law into DEM-based porewater coupling to examine seepage, while Tsuji et al. applied the Darcy–Brinkman equation to DEM in a caisson breakwater setting, simultaneously representing wave-field fluid behavior and porous flow through rubble mounds.

Particle methods, such as ISPH (Incompressible Smoothed Particle Hydrodynamics), also adopt the Darcy–Brinkman equation to unify fluid behavior in porous media, capturing both surface flow and seepage. Coupled ISPH–DEM analyses further combine DEM for soil deformation with ISPH for fluid flow, enabling simultaneous modeling of surface and seepage processes. Within these coupled approaches, the fluid–particle interaction can be handled either by directly integrating pressure forces on individual particles (the "pressure-integral method") or through an empirical drag model (the "drag method"). The pressure-integral method avoids empirical assumptions but demands fluid mesh resolutions significantly finer than the DEM particle size, leading to high computational costs. Ushijima et al. (2017) successfully applied this approach to coarse gravel transport (particle sizes of about 2 cm), but studies with finer particles remain limited.

On the other hand, the drag-type approach treats the fluid as an averaged flow around DEM particles and calculates interaction forces via an empirical drag equation dependent on the relative velocities. This approach requires fluid resolutions on the order of the DEM particle diameter and has been applied by Iwamoto et al. to simulate tsunami-induced deformations in a breakwater rubble mound.

[1] Civil, Human and Environmental Engineering Course of Graduate School of Science and Engineering, Chuo University, 1-13-27 Kasuga, Bunkyo-ku, Tokyo, 112-8551, Japan (Corresponding author)
[2] Department of Civil and Environmental Engineering, Chuo University, 1-13-27 Kasuga, Bunkyo-ku, Tokyo, 112-8551, Japan.

However, DEM-based methods still face practical limitations for large-scale or real-world geotechnical problems. The shape of the modeled particles can significantly affect accuracy, and calibration remains challenging. Consequently, DEM currently lacks broad applicability in capturing the full complexity of real soil behavior.

On the other hand, the particle in cell (PIC) method has recently been proposed as an analysis method that can be applied to large deformations and seepage problems by improving the drawbacks of FEM, DEM, etc. The most representative method among the PIC methods is the MPM (Material Point MPM (Material Point Method) proposed by Sulsky et al. (1994) As shown in Figure 1, the object is modeled as a collection of particles in a Lagrangian manner, and the strain increment is calculated in an Eulerian manner on a grid fixed to the background mesh of particles. The governing equations start from the equations of motion, and the discretization is done by weak formulation using shape functions, so there are many similarities with FEM. In particular, the background mesh allows Eulerian calculations to be performed in the same way as in FEM, making the method highly compatible with FEM. Furthermore, since the deformation of the object is represented as the movement of particles and the background mesh is fixed in space, the mesh constraint for large deformations, as in FEM, can be avoided, and discontinuity behavior can also be represented as the interaction between particles. On the other hand, fundamental soil behaviors induced by hydraulic external forces can be roughly classified into "large deformation/collapse," "permeability," "liquefaction," and "sediment transport". These basic phenomena are combined to cause disasters, but each phenomenon has its own theory and model, and numerical analysis has been conducted focusing on only one of the above phenomena. The reason for this is that there are problems with poor applicability depending on the method selected as the soil discretization method, and problems with poor applicability depending on different assumptions of the governing equations of the soil. Based on the above, this study aims to develop a detailed analysis tool for understanding soil behavior when hydraulic external forces act on the soil.

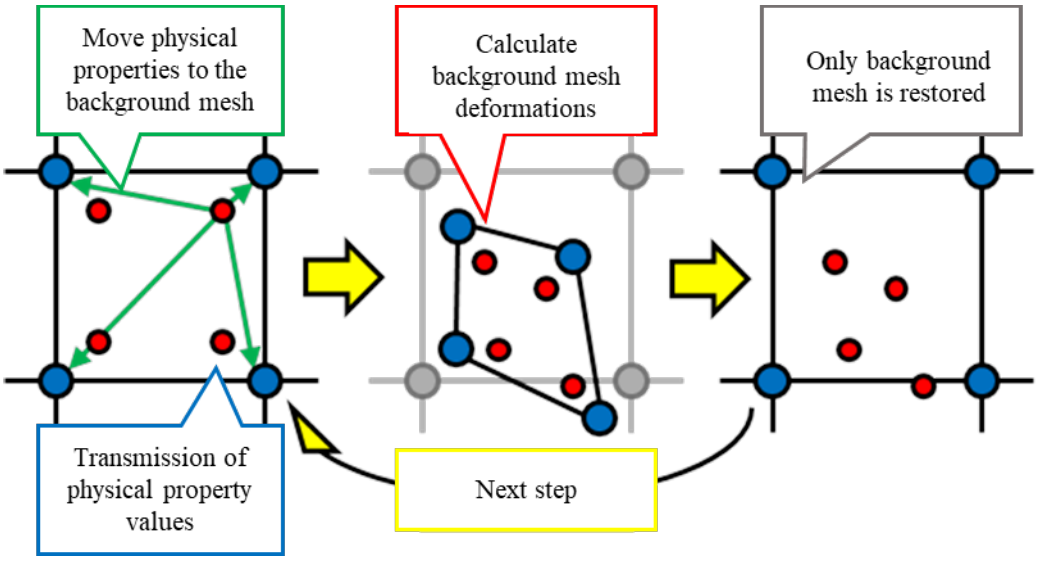

Figure 1. MPM Overview and Calculation Flow.

Method

Figure 2 illustrates the MPM computational workflow, which combines elements of both Lagrangian and Eulerian approaches and falls under the Particle-in-Cell (PIC) method category. In this study, the open-source MPM code Anura3D is employed. Developed by the Anura3D MPM Research Community, Anura3D facilitates solid–liquid two-phase mixture simulations using Biot's u–w formulation. Physical quantities such as mass and momentum are carried by a set of material points, which are updated at fixed time intervals. Through shape function interpolation, these particle-based properties are mapped onto a background mesh that remains spatially fixed, enabling the calculation of nodal velocities by solving the governing equations.

Using these nodal velocities, incremental strains are determined, and the particle positions and physical quantities are updated accordingly. The background mesh then resets to its undeformed state for the subsequent time step, leaving the particles to carry the deformations history. Assuming infinitesimal deformations within each small-time increment, stress increments are derived from the computed strain increments according to a standard elastoplastic constitutive framework. Accumulating these incremental strains yields the total strain in the continuum over the course of the simulation. By iterating this process, MPM successfully captures the large deformations and seepage behaviors characteristic of geotechnical problems.

For the single-phase (solid) model in Anura3D, the fundamental governing equations are derived from the conservation of mass Equation (1) and the conservation of momentum Equation (2).

$$\frac{d}{dt}\rho_s + \rho_s \nabla \cdot v_s = 0 \tag{1}$$

$$\rho_s \frac{dv_s}{dt} = \nabla \cdot \sigma_s + \rho_s b \tag{2}$$

where t is time, ρ_s is the solid phase density, v_s is the solid phase velocity, σ_s is Cauchy's stress tensor, and b is the body force vector. In the liquid one-phase model, the mass and momentum conservation laws are shown in Equation (3) and Equation (4), respectively.

$$\frac{d}{dt}\rho_l + \rho_l \nabla \cdot v_l = 0 \tag{3}$$

$$\rho_l \frac{dv_l}{dt} = \nabla \cdot \sigma_l + \rho_l b \tag{4}$$

where ρ_l is the liquid density, v_l is the liquid velocity, and σ_l is Cauchy's stress tensor. The solid-liquid two-phase model for saturated soil is the mass conservation shown in Equation (5) and the momentum conservation shown in Equation (5).

$$(1-n)\nabla \cdot v_s + \frac{n}{\rho_l}\frac{d\rho_l}{dt} + n\nabla \cdot v_l = 0 \tag{5}$$

$$(1-n)\rho_s \frac{dv_s}{dt} + n\rho_l \frac{dv_l}{dt} = \nabla \cdot \sigma + \rho_{sat} g \tag{6}$$

where n is the porosity, σ is Cauchy's stress tensor, ρ_{sat} is the saturation density, and g is the gravitational acceleration.

The numerical wave modeling software CADMAS-SURF/3D-2F (CS2F), developed by Arikawa et al. (2019), was employed in this study. CS2F uses the Volume of Fluid (VOF) method to capture free-surface flow, with the governing equations comprising the continuity equation for three-dimensional incompressible viscous flow and the Navier–Stokes equations, augmented by a diffusion model for porous media.

For the coupled FDM–MPM procedure, the FDM is responsible for transmitting fluid pressure along the soil surface, while the MPM provides updated soil-particle positions. Specifically, FDM solver passes its time-step and soil surface fluid pressure to MPM, whereas MPM passes porosity information back to the FDM solver. Because MPM often requires a much smaller time increment to ensure stability, the coupled analysis advances in smaller steps on the MPM side.

In the coupled workflow, the first step involves interpolating the mass and velocity carried by each particle onto a background mesh (nodes), using shape functions. The nodal mass and nodal momentum at each no are then computed according to Equations (7) and (8), respectively.

$$m_g^n = \sum_{i=1}^{n_p} S_{i,g} m_p \tag{7}$$

$$M_x^{n-1/2} = \sum_{i=1}^{n_p} S_{i,g} v_p^{n-1/2} \tag{8}$$

Where m is the particle mass, n_p is the number of particles, S is the shape function, M is the momentum, v is the velocity. The subscripts g and p represent the quantities at the node and at the particle, respectively, and n represents the time step. The porosity within the background mesh is also evaluated. Specifically, for each cell in the node, the volume occupied by the cluster of particles—defined by their center positions—is calculated, and this porosity information is sent to the FDM solver at each time step. Subsequently, the equations of motion at the node are solved to determine the background mesh

deformation. The forces acting on the node are expressed as in Equation (9), The external force b_x is determined by the pressure received from FDM from the normal vector and dominant area.

$$f_{x,I}^{n} = \sum_{i=1}^{n_p} \left[S_{i,I} b_x + S_{i,I} m_i g_x + \left(\tau_{xx,i} \cdot \frac{\partial S_{i,I}}{\partial x_g} + \tau_{xy,i} \cdot \frac{\partial S_{i,I}}{\partial y_g} + \tau_{xz,i} \cdot \frac{\partial S_{i,I}}{\partial z_g} \right) V_i^n \right] \tag{9}$$

Where f is the force acting on the node, g is the acceleration of gravity, τ is the stress, V is the volume. The water pressure acting on each mesh is applied as a surface load based on Equation (10).

$$\int_{S_2^e} N_i \boldsymbol{t} ds = \int_{S_2^e} N_i p \boldsymbol{n} ds = \int_{-1}^{1} \int_{-1}^{1} N_i p \boldsymbol{n} |J| \, d\xi d\eta \tag{10}$$

$$r = \begin{Bmatrix} x(\xi,\eta) \\ y(\xi,\eta) \\ z(\xi,\eta) \end{Bmatrix} = \begin{Bmatrix} N_1(\xi,\eta)X_1 + N_2(\xi,\eta)X_2 + \cdots \\ N_1(\xi,\eta)Y_1 + N_2(\xi,\eta)Y_2 + \cdots \\ N_1(\xi,\eta)Z_1 + N_2(\xi,\eta)Z_2 + \cdots \end{Bmatrix} \tag{11}$$

$$r_1 = \frac{\partial r}{\partial \xi} = \frac{\partial}{\partial \xi} \begin{Bmatrix} N_1(\xi,\eta)X_1 + N_2(\xi,\eta)X_2 + \cdots \\ N_1(\xi,\eta)Y_1 + N_2(\xi,\eta)Y_2 + \cdots \\ N_1(\xi,\eta)Z_1 + N_2(\xi,\eta)Z_2 + \cdots \end{Bmatrix} \tag{12}$$

$$r_2 = \frac{\partial r}{\partial \eta} = \frac{\partial}{\partial \eta} \begin{Bmatrix} N_1(\xi,\eta)X_1 + N_2(\xi,\eta)X_2 + \cdots \\ N_1(\xi,\eta)Y_1 + N_2(\xi,\eta)Y_2 + \cdots \\ N_1(\xi,\eta)Z_1 + N_2(\xi,\eta)Z_2 + \cdots \end{Bmatrix} \tag{13}$$

$$n = \frac{r_1 \times r_2}{\|r_1 \times r_2\|} \tag{14}$$

$$|J| = \|r_1 \times r_2\| = \sqrt{\|r_1\|^2 \|r_2\|^2 - (r_1 \cdot r_2)^2} \tag{15}$$

After solving the equations of motion at the nodes, the position and velocity of the particle are updated using equations (16) and (17).

$$x_p^{n+1} = x_p^n + \Delta t \cdot \sum_{I=1}^{n_g} S_{i,g} v_g^{n+1/2} \tag{16}$$

$$u_p^{n+1} = u_p^n + \Delta t \cdot \sum_{I=1}^{n_g} S_{i,g} a_g^{n+1/2} \tag{17}$$

Where x is the particle position, a is the acceleration. The coupled analysis proceeds by looping the above calculations.

2D consolidation problem

To validate the soil–water coupling model developed in this study, two separate one-dimensional consolidation simulations were performed: a solid–liquid two-phase analysis using only Anura3D, and an FDM–MPM coupled analysis. Figure 2 provides an overview of the simulation setup, while Table 1 lists the soil parameters used. In the standalone Anura3D simulation, a saturated soil column (1 m in height) was subjected to a vertical load of $q = 400$kPa. The bottom boundary was fixed, restricting deformation to the vertical direction. To accommodate any upward movement of the saturated soil column, a region free of material points was included above the column.

In the FDM–MPM coupled model, an equivalent water mass ($q = 400$kPa) was applied via the FDM domain above the saturated soil column, mirroring the Anura3D conditions. This setup ensured that fluid pressure at the soil–fluid boundary was transferred to the soil surface. As the saturated column deformed, the position of the soil surface changed accordingly, and the loading point moved with the material points.

Figure 3 compares the time histories of vertical displacement obtained from both the Anura3D solid–liquid two-phase analysis and the FDM–MPM coupled analysis. The results show close agreement between the two simulations. For both approaches, the maximum vertical displacement (approximately 0.211 m) occurred at the topmost material point of the soil column.

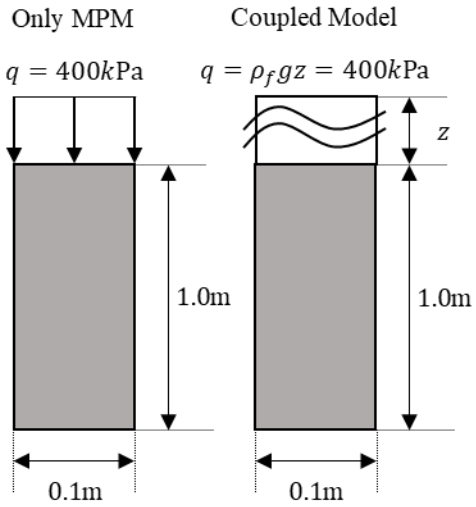

Figure 2. 2D consolidation analysis overview

Table 1. Soil parameters 2D consolidation analysis

Parameter	Symbol	Unit	Value
Initial porosity	n_0	-	0.4
Density solid	ρ_s	kg/m^3	2650
Density liquid	ρ_l	kg/m^3	1000
Permeability	κ	cm/s	1.0×10^{-4}
Bulk modules liquid	K_l	kPa	2.15×10^{4}
Dynamic Viscosity liquid	μ_d	kPa/s	1.002×10^{-6}
Effective Poisson ratio	ν'	-	0.3
Effective Young's modules	E'	kPa	1000
Material model solid: Liner elasticity			

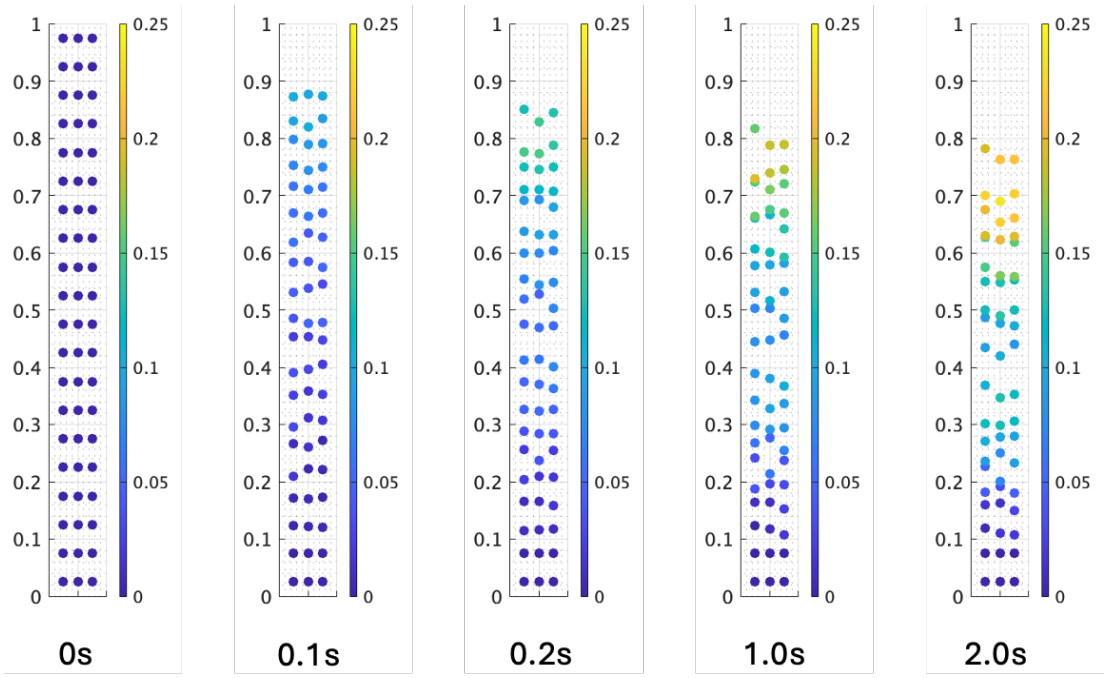

Figure 3(a). Time series of vertical displacement (Only MPM)

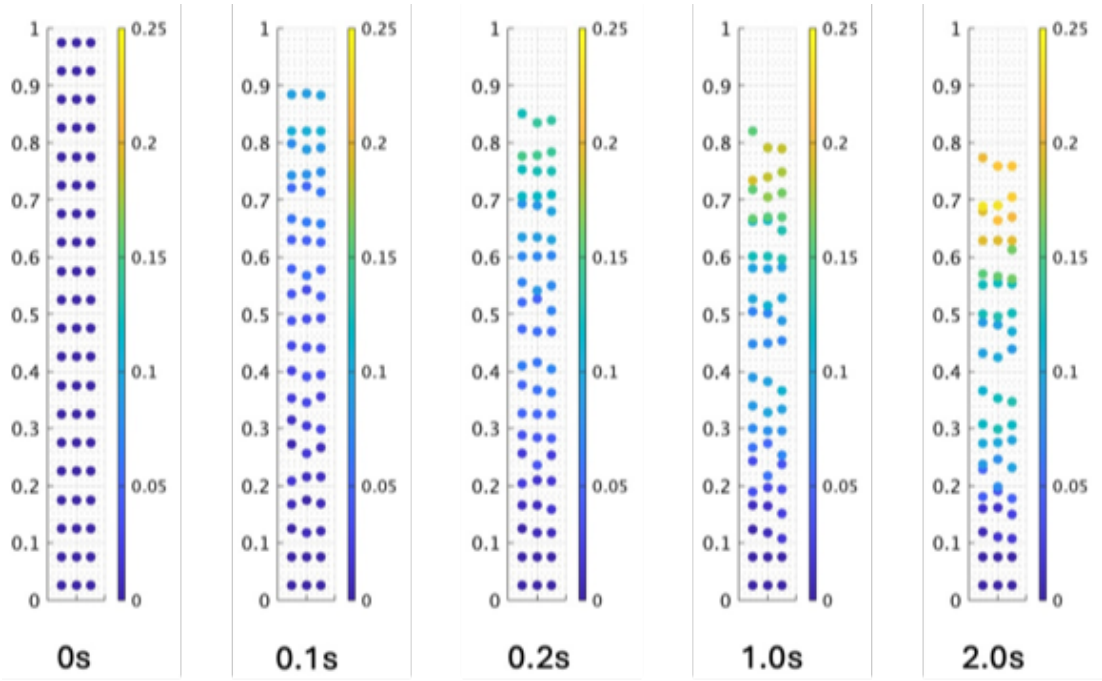

Figure 3(b). Time series of vertical displacement (Coupled model)

2D seepage problem

To validate the model's capability for permeability-related problems, a one-dimensional seepage test was conducted on highly permeable soils previously analyzed by Toyoda and Noda (2017) using the $u-w-p$ formulation. The CADMAS-STR program, which employs the $u-p$ formulation, was also tested to verify the applicability of Biot's equation under a different constitutive framework. Figure 4 provides an overview of the analysis setup, and Table 2 lists the pertinent soil parameters. Time-series data of pore water pressure for various hydraulic conductivities appear in Figure 5. Detailed boundary and loading conditions follow those described by Toyoda and Noda (2017).

For soils with low permeability ($k < 10^{-4}$ cm/s), dynamic effects of seepage are negligible, and the relative motion between soil skeleton and pore fluid remains quasi-static. In contrast, in the higher permeability range ($10^{-3} < k < 10^{-4}$ cm/s), CADMAS-STR ($u-p$ formulation) encountered numerical instability: while the simulation initially ran, it failed after a short time. However, both the $u-w-p$ formulation approach of Toyoda and Noda (2017) and the $u-w$ formulations implemented in Anura3D and CADMAS-MPM successfully handled these highly permeable soils.

For ultra-high permeability ($k > 10^{-1}$ cm/s), the inertia of the pore fluid led to wave-like motion of pore water. Under the $u-w-p$ formulation, this manifested as oscillations in pore water pressure. Notably, these oscillations did not appear in purely $u-w$ models. Although the specific mechanism behind this difference remains unexamined at this stage, similar oscillatory behavior for ultra-high permeability conditions has also been observed in other $u-w$ numerical simulations.

Conclusion

This study proposes a numerical analysis framework for fluid–soil interaction based on the Material Point Method (MPM). By employing the FDM to model fluid flow and MPM to capture soil deformations, a coupled fluid–soil model was constructed. Validation against a one-dimensional consolidation problem demonstrated good agreement between the standalone MPM analysis and the coupled FDM–MPM approach, confirming its effectiveness in tackling large deformations scenarios that are challenging for conventional FEM or DEM techniques. The proposed model holds promise for advancing our understanding of soil behavior under hydraulic forces, such as in liquefaction and landslide events.

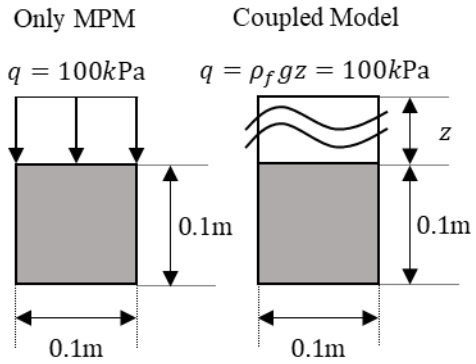

Figure 4. 2D seepage analysis overview

Table 2. Soil parameters 2D seepage analysis

Parameter	Symbol	Unit	Value
Initial porosity	n_9	-	0.4
Density solid	ρ_s	kg/m^3	2650
Density liquid	ρ_l	kg/m^3	1000
Permeability	κ	cm/s	1.0×10^{-7},1.0×10^{-3}, 1.0×10^{-1}
Bulk modules liquid	K_l	kPa	2.15×10^{4}
Dynamic Viscosity liquid	μ_d	kPa/s	1.002×10^{-6}
Effective Poisson ratio	ν'	-	0.35
Effective Young's modules	E'	kPa	1000000
Material model solid: Liner elasticity			

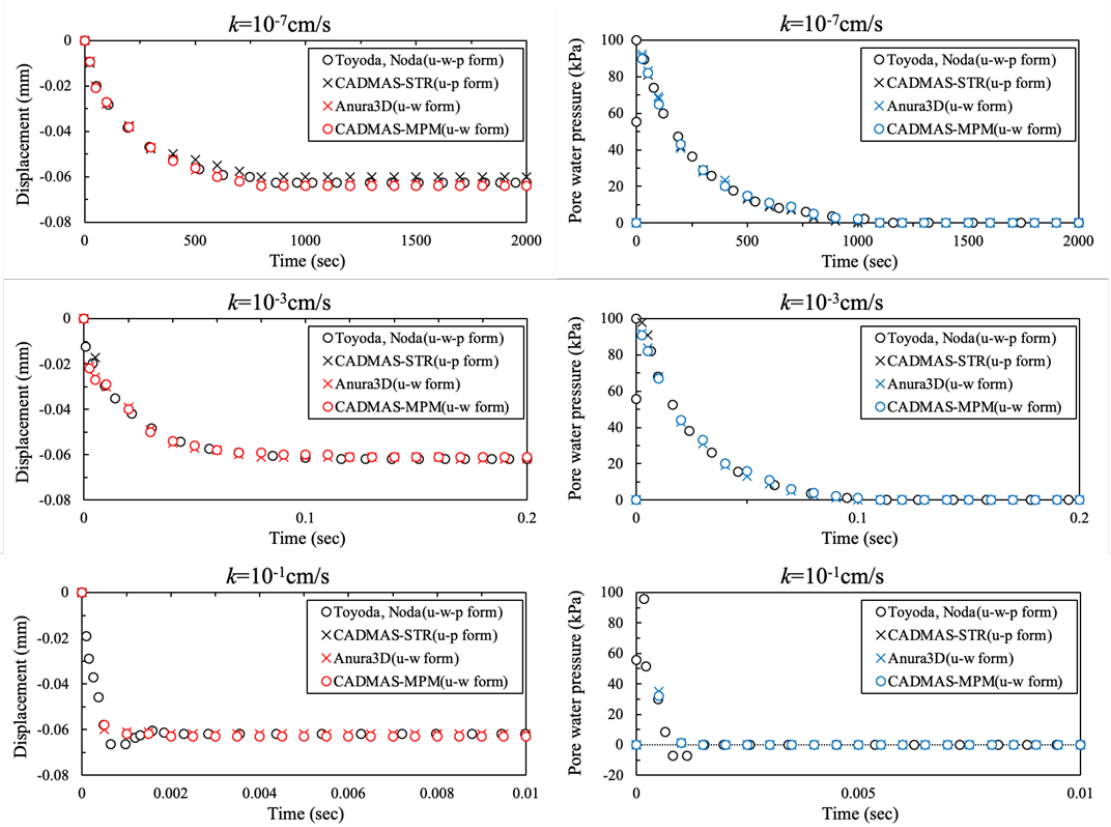

Figure 5. Time series of displacement and pore water pressure (z=0.05m)

REFERENCES

Roscoe, B. E. and Bray, J. D. 1963. Yielding of Clay in States Wetter than Critical, *Geotechnique*, Vol. 13, Issue. 3, pp. 211-240.

Sekiguchi, H. and Ohta, H. 1977. Induced Anisotropy and Time Dependency in Clays, *Proc. 9th, ICSMFE*, Specialty Session 9, Tokyo, pp. 229-238.

Asaoka et al., 2000. Superloading Yield Surface Concept For Highly Structured Soil Behavior, *Soils and Foundations*, Vol. 40, Issue. 2, pp. 99-110.

Kinoshita et al., T. Nishimura, and H. Fujimura 1994. An Advanced Distinct Element Model Coupling With Pore Water, *Proc. of JSCE*, Volume 1994, Issue 499, Pages 31-39.

Tsuji et al., 2021. Seepage Failure Simulation of A Caisson-Type Breakwater Using by ISPH-DEM Coupled Method. *Journal of Japan Society of Civil Engineers*, Ser. A2 (Applied Mechanics (AM)), Volume 77, Issue 2, Pages I_105-I_116.

Ushijima et al., 2017. Computations on Transportations of Gravel Particles Due to Overflows Taking Account of Particle And Particle Fluid Mechanical Interactions, *Journal of Japan Society of Civil Engineers*, Ser. A2 (Applied Mechanics (AM)), Volume 73, Issue 2, Pages I_377-I_386.

Sulsky, D. et al., 1994. A Particle Method for History-Dependent materials, *Computer Methods in Applied Mechanics and Engineering*, Vol.118, pp.179-196.

Iwamoto et al., 2015. Application of Drag Model on SPH-DEM Coupling Analysis Method for the Failures Simulation of Rubble Mound Foundation at a Caisson Breakwater During Tsunami, *Journal of Japan Society of Civil Engineers*, Ser. A2 (Applied Mechanics (AM)), Volume 71, Issue 2, Pages I_579-I_586.

Biot, M.A. 1962. Mechanics of Deformation and Acoustic Propagation in Porous Media. *Journal of Applied Physics*, Vol. 33(4), pp. 1482-1498, 1962.

Hisada, T. and Noguchi, H. 1995. Fundamentals and Applications of Nonlinear Finite Element Method," Maruzen, pp. 24-25.

Noda, T. and Toyoda T. 2019. Development and verification of a soil-water coupled finite deformation analysis based on u-w-p formulation with fluid convective nonlinearity, *Soils and Foundations*, Vol. 59, Issue 4, pp. 888-904.

Uno et al. 2023. Liquefaction Analysis Method by Introducing Governing Equations of Two-Phase System into General-Purpose 3D-FEM, Taisei Advanced Center of Technology Technical Report, No. 56.

Uno H. and Funahara, H., 2022. Improvement in Accuracy of a Soil-Water Coupled Finite Element Analysis Based on the u-U Formulation, Taisei Advanced Center of Technology Technical Report, No. 55.

Toyoda, T. and Noda, T., 2017. A full formulation-based soil-water coupled finite deformation analysis on undrained compression tests on highly permeable soil specimen, *Proceedings of the 19th International Conference on Soil Mechanics and Geotechnical Engineering*, Seoul.

Morimoto et al., 2014. Unified Numarical Analysis Between the Extended Darcy's Law and Navier-Stokes Equation by Using Stabilized ISPH Method, *Journal of Japan Society of Civil Engineers*, Ser. A2 (Applied Mechanics (AM)), Volume 70, Issue 2, Pages I_213-I_221.

Arikawa et al. 2019. Development and Applicability of Multiscale Multiphysics Integrated Simulator for Tsunami, *Journal of Disaster Research*, Vol. 14, No. 2, pp. 225-234.

Anura3D Portal (https://github.com/Anura3D/Anura3D_OpenSource/wiki)